Thermal expansion of single-crystalline β-Ga_2O_3 from RT to 1200 K studied by synchrotron-based high resolution x-ray diffraction

Zongzhe Cheng, Michael Hanke, Zbigniew Galazka, and Achim Trampert

Citation: Appl. Phys. Lett. **113**, 182102 (2018); doi: 10.1063/1.5054265
View online: https://doi.org/10.1063/1.5054265
View Table of Contents: http://aip.scitation.org/toc/apl/113/18
Published by the American Institute of Physics

Sensors, Controllers, Monitors
from the world leader in cryogenic thermometry

Reuse of AIP Publishing content is subject to the terms at: https://publishing.aip.org/authors/rights-and-permissions. Downloaded to: 62.141.165.1 on 01 November 2018, At: 01:39

Thermal expansion of single-crystalline β-Ga_2O_3 from RT to 1200 K studied by synchrotron-based high resolution x-ray diffraction

Zongzhe Cheng,[1] Michael Hanke,[1,a)] Zbigniew Galazka,[2] and Achim Trampert[1]
[1]*Paul-Drude-Institut für Festkörperelektronik, Leibniz-Institut im Forschungsverbund Berlin e.V. Hausvogteiplatz 5–7, 10117 Berlin, Germany*
[2]*Leibniz-Institut für Kristallzüchtung, Max-Born-Straße 2, 12489 Berlin, Germany*

(Received 30 August 2018; accepted 15 October 2018; published online 31 October 2018)

The anisotropic coefficient of thermal expansion for single-crystalline monoclinic β-Ga_2O_3 has been precisely measured by synchrotron-based high resolution x-ray diffraction in the temperature range from 298 to 1200 K. We derived values along the three main crystallographic directions, based on spacings for (600), (020), and $(\bar{2}04)$ lattice planes. α_a changes non-linearly between 0.10×10^{-6} K^{-1} and 2.78×10^{-6} K^{-1} in the temperature range of 298 to 1200 K, while the values of α_b and α_c along the further two directions are nearly double. Within the Einstein model, we have numerically modeled the functional dependencies applying a single phonon mode. *Published by AIP Publishing.*
https://doi.org/10.1063/1.5054265

Ga_2O_3 is a wide-band-gap transparent semiconducting material. It has attracted a lot of attention in the last decade due to its highly promising electrical and optical properties making it the first choice for applications as transparent electrodes,[1] field-effect transistors,[2–5] high power electronics,[6] and solar-blind ultraviolet detectors.[7–9] The rapidly growing interest in this material is evidenced in a 10% increase of publications per year. However, only a few of the basic thermal properties of β-Ga_2O_3 have been addressed in the recent past. An impressive example on how important fundamental properties can be is the paper by Guo *et al.*[10] on anisotropic thermal conductivity. Our work addresses another very basic property of β-Ga_2O_3: its temperature dependent and anisotropic thermal expansion behavior in the window between room temperature (RT) and 1200 K.

Compared with the other polytypes α, γ, δ, and ϵ,[11] the monoclinic β-phase is thermodynamically the most stable at high temperatures, and its epitaxial growth has been achieved in both homo- and heteroepitaxy. As for the homoepitaxy, high quality single crystalline thin films can be coherently deposited on the substrates by different growth methods, such as molecular beam epitaxy (MBE),[12] metalorganic vapor phase epitaxy,[13] and halide vapor phase epitaxy.[14] However, the research on homoepitaxy is possible only to a limited extend due to the limited availability of high quality substrates. Therefore, previous investigations mostly tackled the heteroepitaxial case of β-Ga_2O_3 on foreign substrates, such as α-Al_2O_3,[15,16] Yttrium-stabilized zirconia,[17] and MgO.[18]

Heteroepitaxial lattice mismatch raises stress at the interface and the accumulated strain energy scales with the layer thickness. Beyond a critical value, it might be released by the formation of misfit dislocations.[19] Therefore, lattice mismatch acts as one of the key parameters in heteroepitaxy. Additionally, lattice parameters vary with temperature, whereas the particular functional dependencies are material-specific and anisotropic. In the case of MBE of β-Ga_2O_3 substrate temperatures being substantially higher than RT, typical values are close to 1000 K.[16,20] Annealing processes as well require rather high temperatures.[21] Therefore, precise knowledge on the functional correlation between thermal expansion and temperature covering the entire temperature window between RT and growth temperature becomes mandatory to determine the effective, hence temperature dependent lattice mismatch and the resulting mechanical stress. Previous studies on β-Ga_2O_3 powder and bulk report between 5 and 700 K constant (temperature independent) coefficients of thermal expansion (CTE) along different directions.[22,23]

This letter presents a comprehensive experimental determination of CTE for monoclinic β-Ga_2O_3 by taking into account its temperature dependence from 298 to 1200 K. Lattice plane distances were probed precisely by *in-situ* synchrotron-based high resolution x-ray diffraction. Our experimental findings are simulated within the Einstein model.[24]

All experiments were carried out at the dedicated PHARAO endstation U125/2-KMC at BESSYII (Helmholtz-Zentrum Berlin).[27] This setup enables a direct *in-situ* access to lattice dynamics, since it combines a fully equipped six-circle

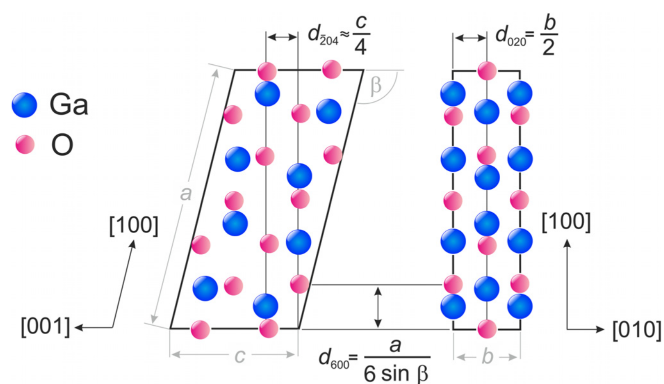

FIG. 1. Crystal structure of β-Ga_2O_3 viewed in [010] (left) and [001] (right) directions. The lattice parameters a, b, and c and their relation to experimentally accessible lattice spacings d for (600), (020), and $(\bar{2}04)$ planes are given. Due to the monoclinic symmetry (i.e., $\beta \neq 90°$), the $\{h00\}$ planes are not perpendicular to the [100] direction. In the right figure, this direction is depicted as projection onto the paper plane. Further on, the surface normal of the $(\bar{2}04)$ planes is tilted by about 0.1° with respect to the [001] direction.

[a)]Electronic mail: hanke@pdi-berlin.de

diffractometer with a custom-built MBE providing ultra-high vacuum (UHV) conditions at a base pressure of about 10^{-10} mbar. There are two x-ray transparent beryllium windows mounted on the growth chamber for the impinging and diffracted x-rays, respectively. The diffractometer allows for both coplanar 2θ-ω and grazing incidence diffraction scattering geometry; therefore, not only out-of-plane but simultaneously also in-plane lattice plane distances are accessible. Angular resolution is provided by a 1 mm slit in front of the detector. A substrate heater manufactured from silicon carbide allows for a temperature window between RT and 1200 K. The beamline is equipped with a Si(111) double-crystal monochromator that defines the x-ray energy at 10 keV with a spectral resolution $\Delta E/E$ of about 10^{-4} and a beam size of approximately $300 \times 500\,\mu\text{m}^2$ at the sample. We have used $5 \times 5 \times 0.5\,\text{mm}^3$ wafers of single-crystalline (100)-oriented β-Ga_2O_3 fabricated from a bulk crystal obtained by the Czochralski method at Leibniz Institute for Crystal Growth in Berlin.[28–30] The wafers were twin-free and electrically insulating.

In order to determine the real temperature of the mounted sample, a (111)-oriented silicon wafer was used to calibrate the thermocouple, since its lattice parameters and CTEs are already well known.[26] Both the silicon substrate and the β-Ga_2O_3 wafers were mounted on the wafer holders by indium bonding, which helps to avoid external stress and further increases the thermal conductivity. The calibration procedure yields a temperature uncertainty of about 10 K above and below the on-site temperature. After the calibration, we have investigated from 298 to 1200 K the temperature dependent diffraction according to lattice spacings d_{hkl} for β-Ga_2O_3, as sketched in Fig. 1. If the angles between the axes are assumed to be constant ($\beta = 103.85°, \alpha = \gamma = 90°$), the respective lattice parameters a, b, and c are given according to $a = 6 \cdot d_{600}/\sin\beta$, $b = 2 \cdot d_{020}$, $c = 4 \cdot d_{\bar{2}04}/\sin 89.9°$.

We want to emphasize that for β-Ga_2O_3 powder, Orlandi *et al.*[23] found a slight increase in the monoclinic angle β by 0.01° when the temperature changes from 300 to 700 K. Assuming a similar behavior for bulk wafers and extrapolating it onto our temperature window, an increase in β by about 0.02° might occur. Hence, this effect on the calculation remains rather small (less than 5% of CTE) and can thus be neglected. According to this assumption, we treat β as a constant value.

The blue squares in Figs. 2(a)–2(c) depict the lattice parameters a, b, and c of bulk β-Ga_2O_3 as a function of wafer temperature T, while the red curves are fits based on the Einstein model. Below each graph, the respective functional dependencies of the various CTEs α_i are plotted as lines together with the constant values for powder.[22,23] Our findings agree with them in the sense that thermal expansion happens anisotropically with $2\alpha_a \approx \alpha_b \approx \alpha_c$. We may note that first principles calculations over a similar temperature range predict about an order of magnitude larger values.[31]

According to the ISO (International Organisation for Standardization) definition of CTE, the coefficient of thermal expansion is given by the following equation:

$$\alpha(T) = \frac{1}{a_{RT}} \frac{da(T)}{dT}, \tag{1}$$

whereby a_{RT} refers to the lattice parameter at RT (around 298 K), and $\frac{da(T)}{dT}$ is the differential lattice parameter over temperature. By neglecting now the influence of the phonon dispersion (i.e., the high temperature regime), $\alpha(T)$ can be calculated according to the Grüneisen equation[32]

$$\alpha(T) = \frac{1}{3}\,\kappa\,\gamma\,C_v(T). \tag{2}$$

Here, γ and κ are the Grüneisen parameter and the harmonic compressibility, respectively. Within the Einstein model, the specific heat C_v of a solid is coupled to its phonons, all of the same frequency but with different occupation probability at various temperatures. With the Einstein temperature θ_E, it yields for the specific heat

$$C_v(T) \propto \left(\frac{\theta_E}{T}\right)^2 \frac{e^{\theta_E/T}}{(-1 + e^{\theta_E/T})^2}. \tag{3}$$

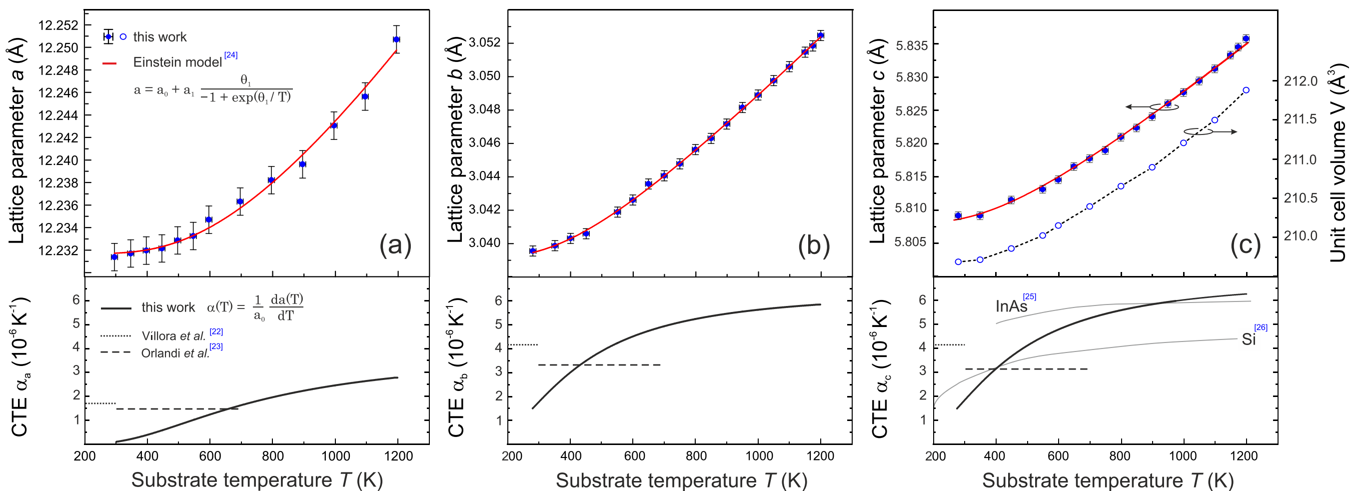

FIG. 2. (a)–(c) Measured lattice parameters a, b, and c and resulting unit cell volume V as a function of temperature T. Red curves show numerical fits applying the Einstein model.[24] The CTEs α_i along the three crystallographic directions [100], [010], and [001] of the monoclinic unit cell are the derivatives of the temperature dependent lattice parameters. They are plotted at the bottom of each figure together with data for β-Ga_2O_3 powder and bulk.[22,23] Numerical values at 298, 600, 800, and 1200 K are listed in Table I. For illustrative purposes, the isotropic values of α for cubic InAs[25] and Si[26] are reproduced in (c).

In a simple model, γ and κ in Eq. (2) can be considered as constants, independent of temperature T. Therefore, $\alpha(T)$ is only proportional to $C_v(T)$, the specific heat per volume. In some cases, e.g., if the CTE is partially negative,[33] a single Einstein-term [as given in Eq. (3)] becomes insufficient and has to be replaced by a summation over m terms

$$\alpha(T) = \frac{1}{a_{RT}} \sum_{k=1}^{m} a_k \left(\frac{\theta_k}{T}\right)^2 \frac{e^{\theta_k/T}}{\left(-1 + e^{\theta_k/T}\right)^2}. \quad (4)$$

Based on that, the lattice parameter can be finally obtained by integration

$$a(T) = a_0 + \sum_{k=1}^{m} a_k \frac{\theta_k}{-1 + e^{\theta_k/T}}. \quad (5)$$

This equation holds for all three considered directions, whereas a_0 refers to the corresponding lattice parameters at RT and the unit of a_k is length per temperature. It is apparent that in Figs. 2(a)–2(c), the simulations based on the Einstein model (the red lines) using a single Einstein-term support very well the discrete data points within the entire temperature window. The respective fitting parameters a_0, a_1, θ_1 for each direction including uncertainties can be found here.[34]

On the basis of the well fitted data, the CTEs can be extracted from the derivative of the thermal expansion. At the bottom of Fig. 2, the CTEs of lattice parameters a, b, and c are plotted as a function of temperature. One interesting feature is that in the probed window, all functions α_a, α_b, and α_c increase with temperature and gradually even approach their high temperature limit close to 1200 K. This is a general saturation effect indicative for fully occupied phonon modes as also observed at, e.g., InAs[25] and Si[26] [cf. Fig. 2(c)]. As for the amplitude of the CTEs, it clearly shows that α_b and α_c follow a rather similar dependency; however, α_a is approximately only half of them. This anisotropic thermal expansion behavior is in correspondence with constant CTEs from 5 to 700 K reported previously.[23] Finally, we would like to mention that the unit cell volume, based on the measured lattice parameters, depicts a similar functional dependence, Fig. 2(c). At the example of four particular temperatures, Table I gives the numerical CTE values.

As for the heteroepitaxy on the c-plane sapphire (α-Al_2O_3) substrate, it has been reported that β-Ga_2O_3 thin films grow along $(\bar{2}01)$-orientation with in-plane rotational domains.[15,16] In those films, the $\{010\}$ planes of β-Ga_2O_3 are parallel with the $\{1\bar{1}00\}$ planes of α-Al_2O_3. The in-plane lattice parameter difference between these two sets of planes at the interface leads to an in-plane lattice mismatch of around 10.65% at RT. Different temperature dependencies of CTE for β-Ga_2O_3 and α-Al_2O_3[35] yield a smaller lattice mismatch at elevated temperatures, as shown in Fig. 3(a). The remaining, however, considerably large value of about 10.40% acts as a key reason for the initial formation of a three-monolayer thin pseudomorphic α-Ga_2O_3 layer before the Ga_2O_3 growth proceeds with its β-phase.[15] In Fig. 3(b), the lattice mismatch between the β-Ga_2O_3 epitaxial film and the α-Ga_2O_3[36] buffer layer is plotted as a function of temperature. It clearly indicates that the lattice mismatch will increase after the growth during the cooling process down to RT. Therefore, it might be important to perform cooling with a rather low rate in order to avoid a fast increase in the lattice mismatch and potential defect formation.

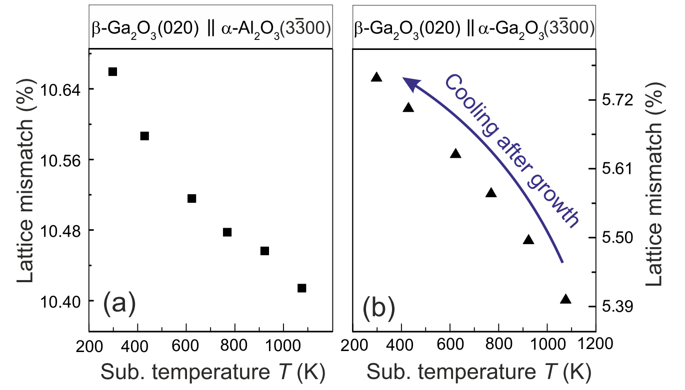

FIG. 3. In-plane lattice mismatch between $(\bar{2}01)$-oriented β-Ga_2O_3 and c-plane sapphire decreases at elevated temperatures (a), similar to the combination β-Ga_2O_3 vs. α-Ga_2O_3 (b).

In summary, the lattice parameters a, b, and c of single-crystalline monoclinic β-Ga_2O_3 bulk were precisely determined by out-of-plane x-ray diffraction and in-plane grazing incidence diffraction in the temperature range from 298 to 1200 K. The experimental results of β-Ga_2O_3 thermal expansion can be modeled applying a single Einstein-term. Our data provide evidence for an anisotropic behavior within the investigated temperature window.

TABLE I. Coefficients of thermal expansion α_a, α_b, and α_c at particular temperatures T for β-Ga_2O_3 bulk as taken from the fitting curves in Figs. 2(a)–2(c). Please note that, according to Eq. (1), α is proportional to the derivative $\frac{da(T)}{dT}$.

	α_a	α_b	α_c
T (K)		(10^{-6} K^{-1})	
RT	0.10	1.68	1.74
600	1.24	4.51	4.79
800	1.97	5.24	5.60
1200	2.78	5.84	6.27

The authors thank Michael Niehle and Martin Schmidbauer for internal reviews of the manuscript and Steffen Behnke for maintaining the MBE system. This work was performed in parts in the framework of GraFOx, a Leibniz ScienceCampus. Providing beamtime at the PHARAO endstation (Helmholtz-Zentrum Berlin) under Grant No. 171-04814 CR/R is highly appreciated.

[1]S. J. Kim, S. Y. Park, K. H. Kim, S. W. Kim, and T. G. Kim, IEEE Electron Device Lett. **35**, 232 (2014).
[2]M. Higashiwaki, K. Sasaki, A. Kuramata, T. Masui, and S. Yamakoshi, Appl. Phys. Lett. **100**, 013504 (2012).
[3]K. D. Chabak, N. Moser, A. J. Green, D. E. Walker, Jr., S. E. Tetlak, E. Heller, A. Crespo, R. Fitch, J. P. McCandless, K. Leedy, M. Baldini, G. Wagner, Z. Galazka, X. Li, and G. Jessen, Appl. Phys. Lett. **109**, 213501 (2016).
[4]A. J. Green, K. D. Chabak, E. R. Heller, R. C. Fitch, M. Baldini, A. Fiedler, K. Irmscher, G. Wagner, Z. Galazka, S. E. Tetlak, A. Crespo, K. Leedy, and G. H. Jessen, IEEE Electron Device Lett. **37**, 902 (2016).

[5]A. J. Green, K. D. Chabak, M. Baldini, N. Moser, R. Gilbert, R. C. Fitch, G. Wagner, Z. Galazka, J. McCandless, A. Crespo, K. Leedy, and G. H. Jessen, IEEE Electron Device Lett. **38**, 790 (2017).
[6]M. Higashiwaki, K. Sasaki, A. Kuramata, T. Masui, and S. Yamakoshi, Phys. Status Solidi A **211**, 21 (2014).
[7]T. Oshima, T. Okuno, and S. Fujita, Jpn. J. Appl. Phys., Part 1 **46**, 7217 (2007).
[8]S. Nakagomi, T. Momo, S. Takahashi, and Y. Kokubun, Appl. Phys. Lett. **103**, 072105 (2013).
[9]D. Guo, Z. Wu, P. Li, Y. An, H. Liu, X. Guo, H. Yan, G. Wang, C. Sun, L. Li, and W. Tang, Opt. Mater. Express **4**, 1067 (2014).
[10]Z. Guo, A. Verma, X. Wu, F. Sun, A. Hickman, T. Masui, A. Kuramata, M. Higashiwaki, D. Jena, and T. Luo, Appl. Phys. Lett. **106**, 111909 (2015).
[11]R. Roy, V. G. Hill, and E. F. Osborn, J. Am. Chem. Soc. **74**, 719 (1952).
[12]Z. Cheng, M. Hanke, Z. Galazka, and A. Trampert, Nanotechnology **29**, 395705 (2018).
[13]G. Wagner, M. Baldini, D. Gogova, M. Schmidbauer, R. Schewski, M. Albrecht, Z. Galazka, D. Klimm, and R. Fornari, Phys. Status Solidi A **211**, 27 (2014).
[14]K. Konishi, K. Goto, R. Togashi, H. Murakami, M. Higashiwaki, A. Kuramata, S. Yamakoshi, B. Monemar, and Y. Kumagai, J. Cryst. Growth **492**, 39 (2018).
[15]R. Schewski, G. Wagner, M. Baldini, D. Gogova, Z. Galazka, T. Schulz, T. Remmele, T. Markurt, H. von Wenckstern, M. Grundmann, O. Bierwagen, P. Vogt, and M. Albrecht, Appl. Phys. Express **8**, 011101 (2015).
[16]Z. Cheng, M. Hanke, P. Vogt, O. Bierwagen, and A. Trampert, Appl. Phys. Lett. **111**, 162104 (2017).
[17]K. Kaneko, H. Ito, S.-D. Lee, and S. Fujita, Phys. Status Solidi C **10**, 1596 (2013).
[18]S. Nakagomi and Y. Kokubun, J. Cryst. Growth **479**, 67 (2017).
[19]K. Kaneko, H. Kawanowa, H. Ito, and S. Fujita, Jpn. J. Appl. Phys., Part 1 **51**, 020201 (2012).
[20]P. Vogt and O. Bierwagen, Appl. Phys. Lett. **108**, 072101 (2016).
[21]H. W. Kim and N. H. Kim, Appl. Surf. Sci. **230**, 301 (2004).
[22]E. G. Víllora, K. Shimamura, T. Ujiie, and K. Aoki, Appl. Phys. Lett. **92**, 202118 (2008).
[23]F. Orlandi, F. Mezzadri, G. Calestani, F. Boschi, and R. Fornari, Appl. Phys. Express **8**, 111101 (2015).
[24]A. Einstein, Ann. Phys. **327**, 180 (1907).
[25]V. M. Glazov and A. S. Pashinkin, Inorg. Mater. **36**, 225 (2000).
[26]Y. Okada and Y. Tokumaru, J. Appl. Phys. **56**, 314 (1984).
[27]B. Jenichen, W. Braun, V. M. Kaganer, A. G. Shtukenberg, L. Däweritz, C.-G. Schulz, K. H. Ploog, and A. Erko, Rev. Sci. Instrum. **74**, 1267 (2003).
[28]Z. Galazka, R. Uecker, D. Klimm, K. Irmscher, M. Naumann, M. Pietsch, A. Kwasniewski, R. Bertram, S. Ganschow, and M. Bickermann, ECS J. Solid State Sci. Technol. **6**, Q3007 (2017).
[29]Z. Galazka, R. Uecker, K. Irmscher, M. Albrecht, D. Klimm, M. Pietsch, M. Brützam, R. Bertram, S. Ganschow, and R. Fornari, Cryst. Res. Technol. **45**, 1229 (2010).
[30]Z. Galazka, K. Irmscher, R. Uecker, R. Bertram, M. Pietsch, A. Kwasniewski, M. Naumann, T. Schulz, R. Schewski, D. Klimm, and M. Bickermann, J. Cryst. Growth **404**, 184 (2014).
[31]M. D. Santia, N. Tandon, and J. D. Albrecht, MRS Adv. **1**, 109 (2016).
[32]H. Ibach, Phys. Status Solidi B **31**, 625 (1969).
[33]T. Middelmann, A. Walkov, G. Bartl, and R. Schödel, Phys. Rev. B **92**, 174113 (2015).
[34]There is a triplet of fitting parameters, [a_0, a_1, θ_1]. Numerical values are [12.2317(3) Å, 4.6(6) $\times 10^{-5}$ Å/K, 2309(240) K], [3.0392(1) Å, 1.94(4) $\times 10^{-5}$ Å/K, 1251(44) K] and [5.8096(2) Å, 4.5(1) $\times 10^{-5}$ Å/K, 1477(59) K] for [100], [010] and [001], respectively.
[35]W. M. Yim and R. J. Paff, J. Appl. Phys. **45**, 1456 (1974).
[36]L. J. Eckert and R. C. Bradt, J. Am. Ceram. Soc. **56**, 229 (1973).